

The Survival of Mafic Magmatic Enclaves and the Timing of Magma Recharge

Philipp Ruprecht¹, Adam C Simon², and Adrian Fiege³

¹University of Nevada, Reno

²University of Michigan

³American Museum of Natural History

November 26, 2022

Abstract

Many intermediate to felsic intrusive and extrusive rocks contain mafic magmatic enclaves that are evidence for magma recharge and mixing. Whether enclaves represent records of pro-longed mixing or syn-eruptive recharge depends on their preservation potential in their intermediate to felsic host magmas. We present a model for enclave consumption where an initial stage of diffusive equilibration loosens the crystal framework in the enclave followed by advective erosion and disaggregation of the loose crystal layer. Using experimental data to constrain the propagation rate of the loosening front leads to enclave “erosion” rates of 10⁻⁵ to 10⁻⁸ cm/s for subvolcanic magma systems. These rates suggest that under some circumstances, enclave records are restricted to syn-eruptive processes, while in most cases enclave populations represent the recharge history over centuries to millennia. On these timescales mafic magmatic enclaves may be unique recorders that can be compared to societal and written records of volcano activity.

Hosted file

essoar.10503477.1.docx available at <https://authorea.com/users/556481/articles/606463-the-survival-of-mafic-magmatic-enclaves-and-the-timing-of-magma-recharge>

1 **The Survival of Mafic Magmatic Enclaves and the Timing of Magma Recharge**

2 **Philipp Ruprecht¹, Adam C. Simon², and Adrian Fiege³**

3 ¹Department of Geological Sciences and Engineering, University of Nevada, Reno, NV, USA.

4 ²Department of Earth and Environmental Sciences, University of Michigan, Ann Arbor, MI,
5 USA.

6 ³Department of Earth and Planetary Sciences, American Museum of Natural History, New York,
7 NY, USA.

8 Corresponding author: Philipp Ruprecht (pruprecht@unr.edu)

9 **Key Points:**

- 10 • Common survival times for mafic enclaves in felsic volcanic systems are centuries to
11 millennia extending timescale records from minerals
- 12 • Mafic enclaves record only syn-eruptive processes in hot magmatic systems
- 13 • Mafic enclaves in plutonic systems may represent recharge histories of 10,000 to 100,000
14 years
15

16 **Abstract**

17 Many intermediate to felsic intrusive and extrusive rocks contain mafic magmatic enclaves that
18 are evidence for magma recharge and mixing. Whether enclaves represent records of pro-longed
19 mixing or syn-eruptive recharge depends on their preservation potential in their intermediate to
20 felsic host magmas. We present a model for enclave consumption where an initial stage of
21 diffusive equilibration loosens the crystal framework in the enclave followed by advective
22 erosion and disaggregation of the loose crystal layer. Using experimental data to constrain the
23 propagation rate of the loosening front leads to enclave “erosion” rates of 10^{-5} to 10^{-8} cm/s for
24 subvolcanic magma systems. These rates suggest that under some circumstances, enclave records
25 are restricted to syn-eruptive processes, while in most cases enclave populations represent the
26 recharge history over centuries to millennia. On these timescales mafic magmatic enclaves may
27 be unique recorders that can be compared to societal and written records of volcano activity.

28 **Plain Language Summary**

29 Two major questions in volcano research are how magma chambers are built through time and
30 how they are disrupted to cause volcanic eruptions. One piece of evidence that chambers are
31 assembled by episodic magma addition from below (called “recharge”) comes from mingled
32 magmas, where mingling is expressed by the presence of two or more chemically distinct
33 magmas. In particular, the more primitive magma in such mingled magmas is commonly present
34 as discrete blobs, called mafic magmatic enclaves. These enclaves are often interpreted as
35 evidence for recharge-triggered volcanic eruptions. However, they may also form during
36 recharge episodes that are not associated with volcanic eruptions and instead only feed and
37 sustain the magma chamber. Here we develop a model that estimates how long mafic magmatic
38 enclaves survive in a chemically-distinct magma chamber to better understand how information
39 drawn from enclaves informs the two major questions above. We find that under most common
40 conditions, they survive for centuries to millennia. Therefore, the presence of enclaves is not
41 explicitly evidence for a recharge-triggered eruption without studying them in greater detail.
42 That detail can then potentially provide information regarding both the run up to eruption as well
43 as magma assembly over centuries and millennia.

44 **1 Introduction**

45 Magma have long been recognized as open systems; a notion supported by abundant
46 signatures in the crystal record and magma (i.e., whole rock) chemistry (e.g., DePaolo, 1981;
47 Davidson et al., 2007; Ruprecht & Wörner, 2007). The most direct evidence is the macroscopic
48 presence of mafic magmatic enclaves (also referred to as quenched mafic inclusions) and crustal
49 and mantle xenoliths (e.g., Bacon & Metz, 1984; Clyne, 1999; Ruprecht et al., 2012). Mafic
50 magmatic enclaves evince incomplete mixing and hybridization where viscosity contrasts during
51 the mixing of felsic and mafic magmas preclude stirring and stretching to the crystal scale and
52 the removal of any macroscopic mixing evidence (Sparks & Marshall, 1986; Ruprecht et al.,
53 2012). However, once mafic magmatic enclaves form, it remains an important question whether
54 they get consumed through time, and if so, how consumption progresses. What is the
55 characteristic timescale associated with enclave-size reduction that controls their long-term
56 presence? The timescale of enclave-size reduction determines if enclaves document
57 predominantly (1) an integrated record of recharge magmas into felsic magma systems or (2)
58 pre- and syn-eruptive changes in intensive parameters of magmatic systems. In the latter case,

59 long-term assembly and end-member contributions can only be inferred from bulk chemistry and
60 individual crystal chemistry.

61 Past work addressing the physical processes of enclave assimilation focused on the
62 survival of macroscopic (ultra-)mafic components in magmas and their incorporation in basaltic
63 magmas. That work suggested that mixed in components get consumed within hours to days of
64 their introduction (Sachs & Stange, 1993; McLeod & Sparks, 1998). Thermal conditions in the
65 hot basaltic magmas and extensive stirring due to the low viscosity of the melts ensure near
66 instantaneous removal of diffusional gradients in the melt. The removal of compositional and
67 thermal gradients drives melting and dissolution, which effectively erases physical evidence of
68 compositionally distinct components. In felsic host magmas, thermal conditions and magma
69 dynamics are also important for enclave survival. For example, mafic magmatic enclaves in
70 plutons provide evidence that enclaves can survive a super-solidus history of a pluton. Yet,
71 plutons often also show extreme macroscopic homogeneity suggesting that homogenization and
72 enclave removal has to occur to some degree given the life time of millions of years for those
73 systems (Coleman et al., 2004). In eruptive magmatic systems that are still stored at elevated
74 temperatures (well above the solidus for periods of time), sufficient energy may be available to
75 partially melt and disaggregate enclaves.

76 A renewed interest has emerged to understand mafic enclave survival in felsic host
77 magmas in response to the growing research that targets magma process timescales, such as
78 mixing, ascent, and eruption (Turner & Costa, 2007). Here, we develop a model for enclave size-
79 reduction combined with data from experiments that juxtapose basaltic andesite and dacitic
80 magmas to explore what controls mafic enclave survival.

81 **2 Field observations related to enclaves and their formation**

82 There are two processes that need to be distinguished when discussing the survival of
83 enclaves: 1) what are the conditions needed for them to form?, and 2) once enclaves form, what
84 is needed to preserve or destroy them? The focus of this paper is on the second question as their
85 formation is controlled by compositional and thermal contrasts (ΔC , ΔT) between recharge and
86 host magma (Marshall & Sparks, 1986), and the dynamics of mixing (Andrews & Manga, 2014;
87 Hodge & Jellinek, 2012; Ruprecht et al., 2012). Ruprecht et al. (2012) argued that while ΔC - ΔT
88 is fundamentally important, the dynamics and physicochemical interaction of mafic with felsic
89 magma leads to time-dependent changes in magma viscosity that can promote enclave formation
90 or allow for effective hybridization with a spectrum between these end-members. In particular,
91 mineral chemistry reveals that, e.g., host magmas can contain enclaves, which contain multiple
92 crystal populations of one or more mineral phases, as well as individual crystals that were
93 themselves disaggregated from enclaves and are preserved in the host (Beard et al., 2005; Martel
94 et al. 2006; Humphreys et al. 2009; Ruprecht et al., 2012). Thus, magmas range from completely
95 hybridized (i.e., no enclaves) to partially hybridized (i.e., host and/or recharge magma have
96 mixed and do not retain end-member compositions, while also containing enclaves) to no
97 microscope/crystal-scale mixing and only mingling in the form of enclaves. In addition to the
98 presence of mafic phenocryst phases being dispersed in host magmas, high anorthite (An)
99 plagioclase microlites interpreted to be of mafic origin (Martel et al., 2006; Humphreys et al.,
100 2009; Ruprecht et al., 2012) suggest that disaggregation is an effective process in removing the
101 macroscopic evidence for mixing. An additional important observation in the microlite record is

102 that their high An cores tend to be rounded, reflecting resorption prior to rim growth of low An
103 plagioclase following the dispersal in the felsic magma (see figure 1 in Martel et al. 2006).

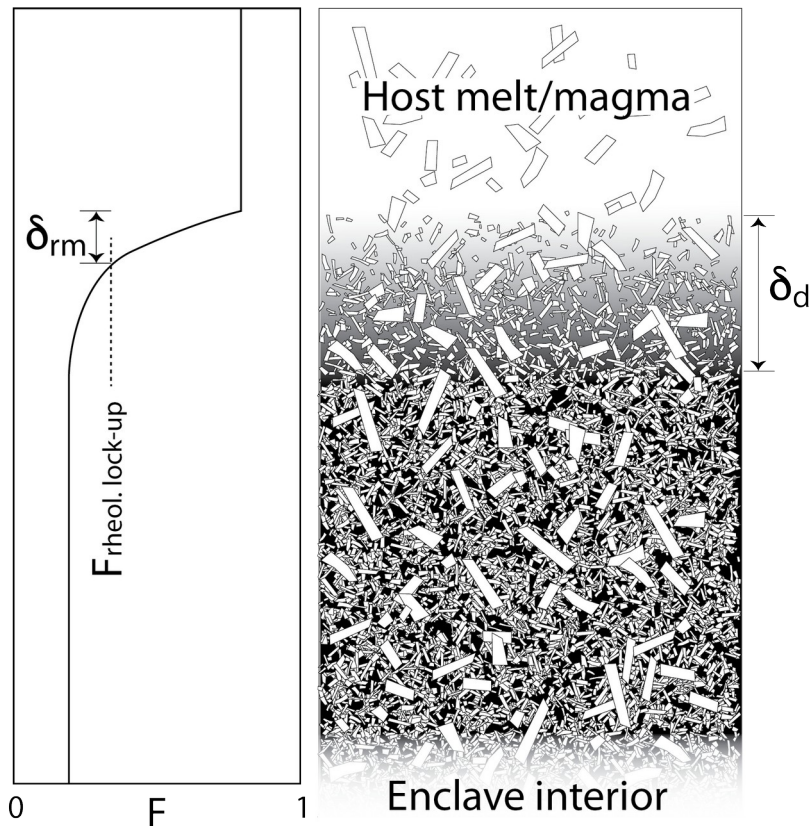
104 Enclave textures can vary drastically and so do the variations in composition and
105 temperature associated with the end-member magmas that drive enclave formation. The range in
106 ΔC and ΔT associated with the two mixing magmas and the relative volume contribution during
107 mixing give rise to a diverse physicochemical and fluid dynamic response that leads to variations
108 in overall crystallinity, a diversity in preserved crystal sizes, as well as the presence and absence
109 of spatial gradients from interiors to enclave rims (e.g., quenched glassy rinds versus more
110 crystalline enclave centers). In general, the significant temperature drop a mafic magma
111 experiences as it comes in contact with cooler felsic host magma generates rapid crystallization
112 of a fine matrix dominated by plagioclase with a subordinate amount of pyroxene, olivine, and
113 oxide (Bacon & Metz, 1984). Second boiling within the enclaves as the enclave crystallizes drive
114 vesiculation and additional plagioclase crystallization leading to many enclaves being almost
115 completely crystallized with interstitial melt pockets making up <40 vol.% of the enclave
116 (Browne et al., 2006). Whether the melt within the enclaves quenches during mixing depends on
117 whether the “race” to the glass transition temperature during cooling is faster than chemical
118 changes to the melt composition related to crystallization, which will lower the glass transition
119 temperature. This race is partially controlled by the thermal evolution during mixing, which is a
120 function of the absolute temperature difference between the mixing magmas and their relative
121 proportion (Ruprecht & Bachmann, 2010). Quenching of the mafic melt is possible if host
122 magmas are close to eutectic temperatures and dominate the mass balance; only in those cases
123 can mafic to intermediate composition melts be quenched and fall below the glass transition
124 temperature (Giordano et al., 2008). The presence of quenched margins in erupted mafic
125 magmatic enclaves may point to fast transport to the surface where quenching can progress
126 rather than quenching in the magma reservoir. Such fast transport is also supported by diffusion
127 profiles in minerals (e.g. Humphreys et al. 2009; Ruprecht and Cooper, 2012). However, if
128 recharge is volumetrically significant, then temperatures of the mixtures are well above any glass
129 transition temperature and crystallization proceeds with the microlite-rich enclaves gaining
130 internal strength as the rheologic lock up is exceeded due to high crystallinity. This latter case is
131 a common occurrence of enclaves and is the focus of this contribution.

132 **3 Physico-chemical processes of enclave consumption**

133 Given the internal strength of a mafic, high-crystallinity enclave (<40% interstitial melt)
134 that develops a crystal framework (Martin et al. 2006), enclave consumption is not simply a
135 function of continued stirring and stretching in the host magma. Instead, the breakup of enclaves
136 requires an interplay of phase change, thus weakening of the internal strength, combined with
137 magma flow driving shear and disaggregation. Previous models focused on the wholesale
138 melting of xenoliths combined with melt flow removing diffusive boundary layers (Sachs &
139 Stange, 1993). However, this process removes any crystal evidence through melting and
140 dissolution of the mafic magma, a condition that is not met for most mixed and mingled magmas
141 that contain abundant enclaves. Instead, individual crystals that originated from a mafic end-
142 member commonly remain dispersed in the host (Clynne, 1999; Browne et al., 2006; Ruprecht et
143 al., 2012). Thus, enclave consumption is the combined process of (a) partial dissolution of
144 microlites and microphenocrysts combined with volatile exsolution that loosens and weakens the
145 crystal framework and (b) melt flow and shear that leads to the detachment of individual crystals
146 or smaller crystal aggregates from the main enclave. Such removal mechanisms may be

147 texturally difficult to identify in natural samples as a few microns to tens of microns can be
 148 sufficient for efficient loosening of the crystal framework.

149 The disaggregation of any aggregate, whether it is silicate minerals or other phases that
 150 are part of a connected cluster of particles, can occur by one of two modes: 1) rupturing where
 151 the new aggregates are reduced in size by a factor on the order of 2 and 2) erosion where shear
 152 and lift forces overcome the attractive forces for individual particles and enclave-size reduction
 153 is controlled by the rate at which individual particles are loosened (progressive dissolution into
 154 the enclave) and by the relative movement of enclave and surrounding melt (Powell & Mason,
 155 1982; Ottino et al., 1999). Loosening of the particle framework happens in response to chemical
 156 disequilibrium between the host magma and the mineral assemblage in the mafic enclave. In
 157 particular, the plagioclase microlites that grow in response to cooling and second boiling during
 158 enclave formation are vulnerable to partial dissolution. Given that they make up most of the
 159 framework that holds enclaves together, it is their dissolution that ultimately leads to the erosion
 160 of the enclave and the release of mafic phenocrysts to the host magma (Fig. 1).



161

162 **Figure 1.** Conceptual model of enclave consumption and general model describing our
 163 underlying experiments (Figure 2A). If temperature conditions are such that enclave minerals
 164 (most importantly plagioclase, which is the only phase shown for simplicity) are melted, a
 165 boundary layer (δ_d) forms that is diffusion controlled and advances following $\sqrt{(Dt)}$. Within a
 166 convective regime, the boundary layer δ_d will be reduced by δ_{rm} , which is the instantaneous
 167 removal of material with crystallinity below the rheologic lock-up. Mafic plagioclase (and other)
 168 phenocrysts will be added to the host melt. F is the melt fraction with the rheologic lock-up melt
 169 fraction ranging between 0.4 and 0.6.

170 Our model for enclave consumption is therefore twofold and starts after enclaves have
 171 formed and established a textural framework that includes phenocrysts, microlites, melt, and
 172 volatile bubbles in response to the local thermal equilibration of mafic and felsic magma.
 173 Dissolution advances into the enclave, which increases the interstitial melt fraction in the enclave
 174 above the rheologic lock-up ($>0.4-0.6$; Marsh, 1989). This is a diffusive process with a
 175 characteristic square-root relationship between length- and time-scale, and has been described
 176 previously (Tsuchiyama, 1985; 1986; Sachs & Stange, 1993; McLeod & Sparks, 1998). The
 177 physical removal of the emerging low-crystallinity boundary layer then occurs in a second step
 178 that is instantaneous as soon as the melt fraction decreases below rheologic lock-up. The exact
 179 conditions that govern the switch between diffusion-controlled plagioclase microlite dissolution
 180 and advection-driven removal of the boundary layer remains poorly constrained as such
 181 boundary layer problems have yet to be studied in much greater detail (Ottino et al., 1999). We
 182 assume diffusion operates first for timescales T_L such that individual plagioclase microlites
 183 become sufficiently loose to be removed from the enclave or crystal aggregate. Once T_L is
 184 reached, enough loosening of the crystal network has occurred and the boundary layer is
 185 removed by advection. The advective-driven size reduction is therefore a function of lengthscale
 186 δ_{rm} associated with T_L . The lengthscale of enclave consumption is thus best described by a
 187 diffusive-advective model:

$$188 \quad x(t) = k\sqrt{t} \text{ for } t < T_L ; \quad \text{Eq. 1}$$

$$189 \quad \delta_{rm}(T_L) = k\sqrt{t} \text{ for } t = T_L ; \quad \text{Eq. 2}$$

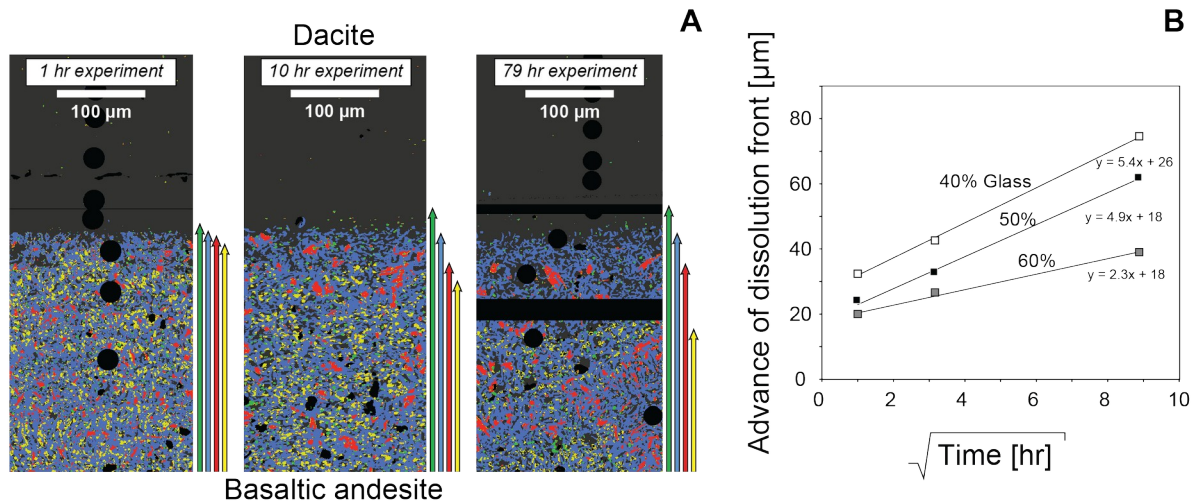
$$190 \quad x(t) = k_L t \text{ for } t > T_L ; \quad \text{Eq. 3}$$

191 With $k_L = \delta_{rm}/T_L$, where T_L is the time to reach a localized (crystal-scale) melt fraction that
 192 exceeds the rheologic lock-up and k_L is the dissolution rate when the advective regime takes over.

193 **4 Experimental constraints on microlite dissolution and advective-controlled erosion rates**

194 Our model is motivated by recently published time series experiments that explore the
 195 physico-chemical processes at mafic-felsic magma interfaces (Fiege et al., 2017; for more details
 196 of these experiments see also the supporting information). The experiments were conducted at
 197 1,000 °C and are especially relevant for cases where the mass balance ratio of mafic recharge to
 198 host magma is large. The experiments exhibit the development of a systematic dissolution front
 199 in the mafic magma that is extensively crystallized with microlite-size plagioclase and
 200 subordinate mafic minerals and oxides (Fig. 2A). Analysis of the advancement of this dissolution
 201 front reveals a square root relationship (consistent with Eq. 1 of our model) that holds for a range
 202 of potential lock-up melt fractions (0.4-0.6; Fig. 2B).

203

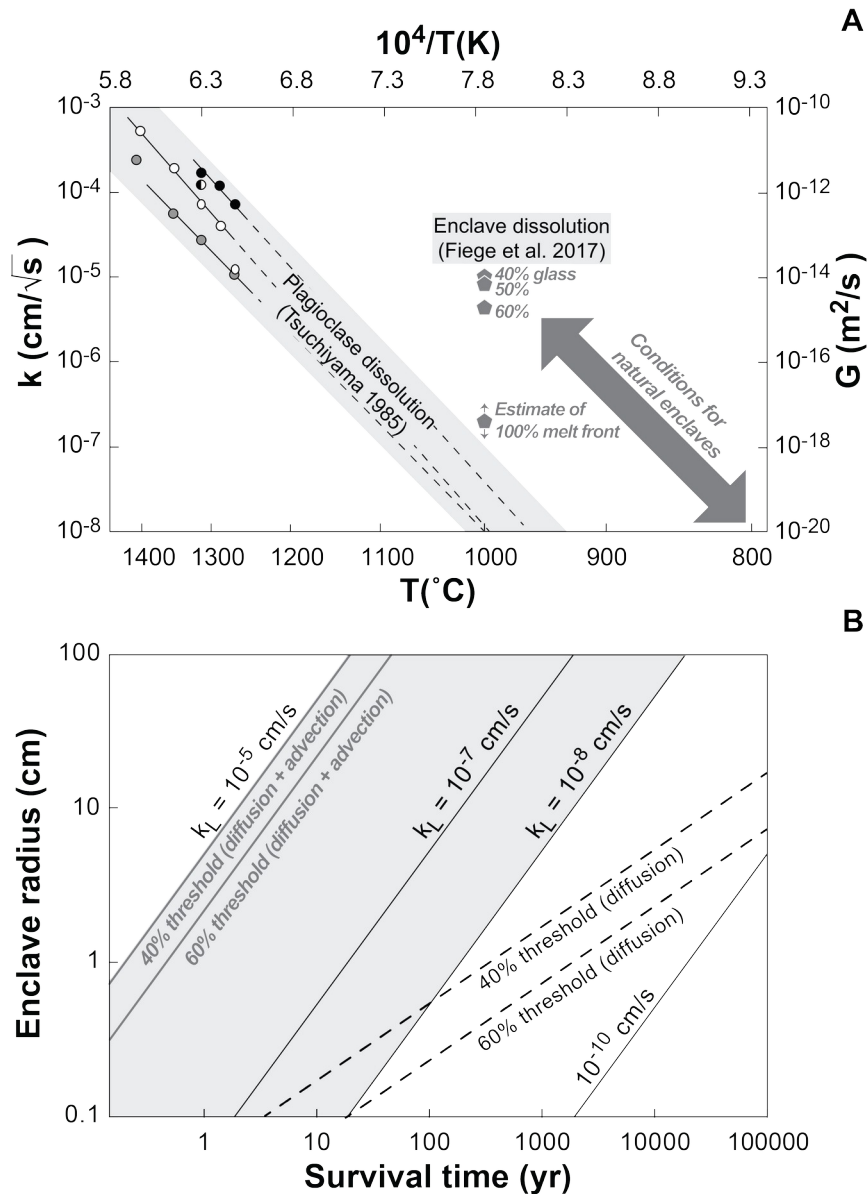


204

205 **Figure 2.** A) False color wavelength-dispersive X-ray maps from the timeseries experiments of
 206 Fiege et al. (2017). Gray: Silicate glass, green: spinel, blue: plagioclase, red: orthopyroxene,
 207 yellow: clinopyroxene. The arrows next to each map indicate the presence of the respective
 208 mineral phase in the basaltic andesite. B) Estimated advance of the dissolution front within the
 209 basaltic andesite of the three timeseries experiments. Mineral fractions change according to
 210 simple diffusion-controlled scaling. The basaltic andesite becomes progressively glass-rich
 211 through time documented by the advancing front of 40, 50, and 60% glass. The non-zero
 212 intercept is either a result of imprecise locating of the interface or due to heating rate effects. For
 213 more information on the image processing and associated uncertainties see extended data
 214 presentation in the supplement.

215

216 The crystal dissolution rates determined from these experiments are faster than
 217 experiments that measured the dissolution rate of a large plagioclase crystal at high temperature.
 218 (Tsuchiyama, 1985; Fig. 3a). Comparison is difficult for two reasons. First, previous experiments
 219 looked at 1D dissolution of individual, large plagioclase crystals in diopside-albite-anorthite
 220 melts at >1200 °C, while our experiments are poly-mineral aggregates dominated by plagioclase
 221 with a large surface area of melt-plagioclase contact (Fig. 2A). Second, our experiments are
 222 performed at lower temperatures, more realistic for natural systems, while being placed in large
 223 chemical disequilibrium. When we estimate the evolution of the 100% melt front, our rates are
 224 comparable to the ones from Tsuchiyama (1985). However, we argue above (section 3) that
 225 100% dissolution is not required for enclave consumption.



226

227 **Figure 3.** A) Comparison of poly-mineral experiments that include plagioclase dissolution (Fiege
 228 et al. 2017) with single crystal dissolution rates by Tsuchiyama (1985). Gray pentagons are the
 229 slopes in figure 2. The advancement of the 100% melt front is estimated from experiments in
 230 Fiege et al. (2017), but spatial scales for these experiments are too short to constrain the rates
 231 with low uncertainties. A conversion to a conventional diffusion rate G is provided. B) Enclave
 232 erosion and survival times for a range of advective “erosion” rates. Assuming that advection
 233 becomes important within hours of diffusion-controlled dissolution provides an estimate for the
 234 rates of advective removal (k_L). Conditions for natural systems suggest advective removal rates
 235 between 10^{-5} to 10^{-8} cm/s. For comparison, enclave survival in the absence of advection (dashed
 236 lines) is shown for rates derived from experiments by Fiege et al. (2017).

237

238 These experimental results allow us to explore the timescale(s) of enclave survival that
239 significantly exceed the timescales for pure melting under hot basaltic conditions, and provide
240 some constraints on enclave survival and preservation. Our results (Fig. 2 and 3a) indicate that
241 the diffusive front for 40-60% melt advances at 10^{-5} to 10^{-6} cm/ \sqrt{s} (equivalent to 10^{-14} to 10^{-16} m²/s
242 when cast as a more conventional diffusion/dissolution rate G). Such rates are likely limited to
243 high temperatures that are reached for rare cases where mafic input is large and the system is
244 thermally re-equilibrating slowly to more intermediate temperature conditions. It therefore
245 represents a case for the more rapid consumption of mafic magmatic enclaves. More moderate
246 conditions, where magmas may experience temperatures and plagioclase dissolution at 800-900
247 °C are more common for many andesitic to dacitic systems (Murphy et al., 2000; Holtz et al.,
248 2005; Ruprecht et al., 2012) and those conditions may persist for longer timescales.
249 Extrapolating rates from the experiments by Tsuchiyama (1985) and Fiege et al. (2017) suggest
250 diffusion-controlled rates of 10^{-7} to 10^{-8} cm/ \sqrt{s} ($\rightarrow G = 10^{-18}$ to 10^{-20} m²/s) for temperatures of 800-
251 900 °C. If one assumes that advective processes take over within hours of diffusion-controlled
252 dissolution, we can estimate the advection-controlled removal rate k_L to vary between 10^{-5} to 10^{-}
253 ⁸cm/s for common andesitic to dacitic systems that frequently erupt mingled magmas with cm- to
254 dm-size enclaves (Fig. 3b and Eq. 3). Such rates imply that enclaves consumed by an erosive
255 process survive no longer than 100 to 1000 years. Any additional size reduction process, e.g., by
256 rupturing, which is sometimes recorded in volcanic and plutonic systems and results from melt
257 infiltration and the presence of large stresses (Laumonier et al., 2014), further reduces the
258 survival times. Of course, enclave survival is also a function of enclave sizes (Fig. 3). Our model
259 implies that if erosion is the dominant process, survival times are directly proportional to enclave
260 size. Thus, systems with very large mafic magmatic enclaves (e.g., 1 m radius) may survive
261 significantly longer. However, field evidence in the form of partially-ruptured enclaves,
262 abundant specifically in larger enclaves, suggests that size-reduction by rupture is enhanced in
263 the larger enclaves and, therefore, even those may quickly get reduced to sizes where erosion
264 dominates.

265 5 Discussion

266 Once conditions are met for enclave formation, the question is whether they will survive
267 past the lifetime of the magmatic system or whether they become part of a hybridized mixture
268 through time. Those conditions may be met during many recharge events, which are likely to
269 occur on the order of every tens to hundreds of years (Ruprecht & Wörner, 2007). Moreover,
270 residence times of long-lived magma bodies in the crust often exceed 100 kyr (Reid et al., 1997).
271 Thus, if survival exceeds the lifetime of the magmatic system, erupted magmas should be full of
272 different enclave populations in magmatic systems that juxtapose evolved host and primitive
273 recharge magmas in the crust. Even if recharge magmas are similar over such timescale, it is
274 plausible to envision large diversity in enclave textures and compositions. While diversity is
275 present in enclaves in many evolved lavas, they typically show only the presence of a few
276 different populations (Clynne, 1999; Browne et al., 2006). One potential explanation is that
277 enclaves are removed from the magma system through time. The survival of dispersed enclaves
278 in magmas is important because if enclaves survived indefinitely, they could be used to
279 understand the long-term assembly of magmatic systems. If they are lost relatively quickly from
280 the rock record then enclave populations may provide important information on just the pre-
281 eruptive changes in the magmatic system.

282 Enclave removal may occur through settling. While some field evidence in plutons
283 suggests that enclaves may settle under some recharge conditions and internal dynamics of the
284 magma body (Wiebe & Collins, 1998), plutonic records are inconsistent with efficient wholesale
285 removal and deposition. Despite the greater density of mafic magmatic enclaves relative to the
286 surrounding evolved magma, any minor convection in a viscous magma will keep them in
287 suspension over long times as they either drift in the magma or operate as passive tracers
288 (Burgisser et al., 2005). Further, in water-rich magmatic systems, enclaves are often vesiculated,
289 and the exsolved volatile phase imparts buoyancy to the enclaves and inhibits settling. We
290 therefore argue that only the largest enclaves can easily be lost by settling. The majority of cm-
291 to dm-size enclaves remain dispersed in the host magma for extended times and interact with
292 host magma with which they are not in equilibrium.

293 Under some thermal conditions enclaves may become macroscopically largely
294 unrecognizable because they deform viscously into thin sheets during magma transport. Such
295 flattening has been observed in nature (e.g. in the Adamello batholith; John & Blundy, 1993).
296 However, the formation of magmatic fabric that erases enclave records require substantial flow
297 (Paterson et al. 1998) and therefore is not an effective mechanism to completely erase a
298 macroscopic record of mafic magmatic enclaves. This was recently tested numerically (Burgisser
299 et al., 2020). Deformation is most effective during initial mafic-felsic interaction and enclave
300 formation (Hodge & Jellinek, 2012; Andrews & Manga 2014) after that viscous deformation
301 may sometimes lead to textures that resemble flow banding, but it is unlikely to completely erase
302 the macroscopic record of mixing and enclave formation throughout the rock.

303 Alternatively to settling and viscous deformation, the thermodynamic disequilibrium in
304 which enclaves find themselves may drive complete melting and dissolution. Mineral chemistry
305 is often still significantly out of equilibrium with respect to an evolved melt (e.g., high An
306 content plagioclase) and such minerals can respond to this disequilibrium by melting and
307 dissolution; this is particularly common for plagioclase and even visible in microlites (Martel et
308 al. 2006). However, if dissolution and melting was the lone process in removing the enclave
309 record, then no crystals of the recharge magmas should survive, which is inconsistent with field
310 observations (Clynne, 1999; Beard et al., 2005; Browne et al., 2006; Humphreys et al., 2009;
311 Ruprecht et al., 2012). Instead, we argue that enclave survival times are controlled by a
312 combination of dissolution and physical disaggregation. Here, dissolution is especially effective
313 on the small microlites with large surface-to-volume ratios that experience a significant size
314 reduction and that can be liberated easily from an enclave or any other crystal-rich aggregate,
315 while preserving the larger phenocrysts. The stage of loosening by dissolution is important as it
316 promotes the complete disintegration of enclaves to individual minerals. If disaggregation alone
317 operates on the enclaves, then we would expect that micro-enclaves persist much longer as
318 stresses on the enclave during stretching and stirring diminish with the crystal cluster size. While
319 micro-enclaves in the form of glomerocrysts and crystal clusters have been described in various
320 studies, they are subordinate to the dispersal of individual microlites (Martel et al., 2006;
321 Humphreys et al., 2009; Ruprecht et al., 2012).

322 As a result, survival times in volcanic systems may be as short as a few years ($k_L \sim 10^{-5}$
323 m/s; mingling under hot conditions and small enclave sizes). Thus, in very hot systems, enclaves
324 potentially only record the lead up to- and syn-eruptive history. In more moderate subvolcanic
325 conditions our model suggests centuries to millennia for their complete removal ($k_L \sim 10^{-7}$ to 10^{-8}
326 m/s). Such survival times are consistent with a partial record of recharge preserved by mafic

327 magmatic enclaves. Most intermediate to evolved magmatic systems that erupted magmas with
328 mafic magmatic enclaves therefore provide more than syn-eruptive process information. Instead,
329 multiple populations of enclaves may constrain compositional diversity that is being added to the
330 magma system over centuries and millennia instead of a complex history of syn-eruptive magma
331 assembly. By detailed bulk and mineral analysis of these populations we may be able to study
332 the lead up to an eruption in greater detail as individual populations may represent different time
333 markers in the lead up history. As a result, they also potentially extend temporal records from
334 crystals to longer timescales as they add the timescale of disintegration to mineral equilibration.
335 Moreover, such timescales suggest that for many magmatic systems mafic magmatic enclaves
336 represent an integrated record over multiple eruptions and therefore they may be uniquely
337 sensitive to providing constraints on the cycling in between eruptions. However, mafic magmatic
338 enclaves are unlikely to provide a meaningful record of the entire recharge history for long-lived
339 magma systems.

340 Whether reactive processes at the interface of mafic magmatic enclaves described here
341 are also important in the plutonic record is complicated by the prolonged cooling recorded in
342 plutons. The reactive process occurs shortly after mingling and if it is not completed (i.e.,
343 enclaves are disintegrated), any reactive front will be overprinted in the plutonic record and
344 reactive boundary layers will be difficult to preserve or to infer. In some cases glassy rinds do
345 survive (Wiebe 2016) and suggest that the mafic-felsic mass ratio and temperature difference are
346 so that glass transition temperatures are reached. However, there are also examples of reactive
347 boundary layers in plutonic settings regarding mafic enclaves. They involve gradual changes in
348 texture and chemistry, as well as rinds rich in, e.g., biotite (Chen et al., 2009; Farner et al., 2014;
349 Michel et al., 2017). Thus, extrapolating dissolution rates to temperatures of long-term storage
350 conditions of plutons is difficult. Advective erosion rates are likely much smaller (potentially k_L
351 $< 10^{-10}$ m/s). We can only speculate on timescales of enclave survival in plutonic systems. For
352 advective erosion rates of 10^{-10} m/s, we predict that many episodes of enclave formation are
353 erased over a plutons prolonged live and only enclaves produced through recharge within the last
354 10,000 to 100,000 years are preserved.

355 **6 Conclusions**

356 Given the current view that magma systems grow incrementally by a complex interplay
357 of recharge, differentiation, assimilation, and melt segregation (Bachmann & Bergantz, 2004;
358 Coleman et al., 2004; Hildreth et al., 2004), it suggests that either not all recharge is mafic and
359 some systems experience recharge only in the form of evolved magmas, or that mafic recharge is
360 often hybridized effectively and only individual crystals provide testimony to the open system
361 behavior. Nonetheless, given that mafic recharge is central – why do we not see more evidence
362 for mafic magmatic enclaves? They are present in some lavas, but just as common is their
363 absence. Some plutons have no enclaves, whereas others contain abundant enclaves, and even
364 others only have zones of mafic magmatic enclaves. This suggests that they are only partially
365 retained – that processes lead to their removal. Our model is consistent with this notion. If partial
366 retainment of enclaves is the dominant mode of preservation, enclaves lend themselves as unique
367 components in magmatic systems to study the magma assembly and build up to eruptions on
368 timescales of centuries to millennia, complementing the short record often retained in mineral
369 diffusion studies (Costa & Chakraborty, 2004; Shamloo & Till, 2019) and long-term integrated
370 record of plutons (Paterson et al., 2016). The presence of enclaves cannot be explicitly used as
371 evidence for a recharge-triggered eruption without additional constraints. While timescales from

372 individual crystals can be reconciled with modern continuous monitoring signals, we suggest that
 373 detailed investigation and extraction of timescales from enclave populations can be reconciled
 374 with historic and societal records of volcano activity.

375

376 **Acknowledgments**

377 We gratefully acknowledge the constructive reviews by J. Blundy and V. Memeti as well
 378 as the thought-provoking discussions and comments by G. Bergantz and M. Clynne. PR (EAR
 379 1250414/1707615) and ACS (EAR 1250239/1524394/1924142) acknowledge funding from the
 380 US National Science Foundation. Data for figure 2B and S1B are available at doi:
 381 10.1594/IEDA/111480.

382 **References**

- 383 Andrews, B.J., & Manga, M. (2014), Thermal and rheological controls on the formation of mafic
 384 enclaves or banded pumice. *Contrib Mineral Petrol*, 167, 961. doi: 10.1007/s00410-013-0961-7
- 385 Bachmann, O., & Bergantz, G.W. (2004), On the Origin of Crystal-poor Rhyolites: Extracted
 386 from Batholithic Crystal Mushes. *J. Petrology*, 45, 1565–1582.
- 387 Bacon, C.R., & Metz, J. (1984), Magmatic inclusions in rhyolites, contaminated basalts, and
 388 compositional zonation beneath the Coso volcanic field, California. *Contributions to Mineralogy
 389 and Petrology*, 85, 346–365. Doi: 10.1007/BF01150292
- 390 Beard, J.S., Ragland, P.C., & Crawford, M.L. (2005), Reactive bulk assimilation: A model for
 391 crust-mantle mixing in silicic magmas. *Geology*, 33, 681–684.
- 392 Browne, B.L., Eichelberger, J.C., Patino, L.C., Vogel, T.A., Dehn, J., Uto, K., & Hoshizumi, H.
 393 (2006), Generation of Porphyritic and Equigranular Mafic Enclaves During Magma Recharge
 394 Events at Unzen Volcano, Japan. *J. Petrology*, 47, 301–328. doi: 10.1093/petrology/egi076
- 395 Burgisser, A., Bergantz, G.W., & Breidenthal, R.E. (2005), Addressing complexity in laboratory
 396 experiments: the scaling of dilute multiphase flows in magmatic systems. *J Volcanol Geothermal
 397 Research*, 141, 245–265.
- 398 Burgisser, A., Carrara, A., & Annen, C. (2020), Numerical simulations of magmatic enclave
 399 deformation. *Journal of Volcanology and Geothermal Research*, 392, 106790. doi:
 400 [10.1016/j.jvolgeores.2020.106790](https://doi.org/10.1016/j.jvolgeores.2020.106790)
- 401 Chen, B., Chen, Z.C., & Jahn, B.M. (2009), Origin of mafic enclaves from the Taihang Mesozoic
 402 orogen, north China craton. *Lithos*, 110, 343–358. doi: [10.1016/j.lithos.2009.01.015](https://doi.org/10.1016/j.lithos.2009.01.015)
- 403 Clynne, M.A. (1999), A complex magma mixing origin for rocks erupted in 1915, Lassen Peak,
 404 California. *J. Petrology*, 40, 105–132.
- 405 Coleman, D.S., Gray, W., & Glazner, A.F. (2004), Rethinking the emplacement and evolution of
 406 zoned plutons: Geochronologic evidence for incremental assembly of the Tuolumne Intrusive
 407 Suite, California. *Geology*, 32, 433–436.
- 408 Costa, F., & Chakraborty, S. (2004), Decadal time gaps between mafic intrusion and silicic
 409 eruption obtained from chemical zoning patterns in olivine. *Earth and Planetary Science Letters*,
 410 227, 517–530.

- 411 Davidson, J.P., Morgan, D.J., Charlier, B.L.A., Harlou, R., & Hora, J.M. (2007), Microsampling
412 and isotopic analysis of igneous rocks: Implications for the study of magmatic systems. *Annu.*
413 *Rev. Earth Planet. Sci.*, 35, 273–311.
- 414 DePaolo, D.J. (1981), Trace element and isotopic effects of combined wallrock assimilation and
415 fractional crystallization. *Earth and Planetary Science Letters*, 53, 189–202.
- 416 Farner, M.J., Lee, C.-T.A., & Putirka, K.D. (2014), Mafic–felsic magma mixing limited by
417 reactive processes: A case study of biotite-rich rinds on mafic enclaves. *Earth and Planetary*
418 *Science Letters*, 393, 49–59. doi: [10.1016/j.epsl.2014.02.040](https://doi.org/10.1016/j.epsl.2014.02.040)
- 419 Fiege, A., Ruprecht, P., & Simon, A.C. (2017), A magma mixing redox trap that moderates mass
420 transfer of sulfur and metals. *Geochemical Perspective Letters*, 3, 190–200. doi:
421 [10.7185/geochemlet.1722](https://doi.org/10.7185/geochemlet.1722)
- 422 Giordano, D., Russell, J.K., & Dingwell, D.B. (2008), Viscosity of magmatic liquids: A model.
423 *Earth and Planetary Science Letters*, 271, 123–134. doi: [10.1016/j.epsl.2008.03.038](https://doi.org/10.1016/j.epsl.2008.03.038)
- 424 Hildreth, W. (2004), Volcanological perspectives on Long Valley, Mammoth Mountain, and
425 Mono Craters: several contiguous but discrete systems. *Journal of Volcanology and Geothermal*
426 *Research*, 136, 169–198.
- 427 Hodge, K.F., & Jellinek, A.M. (2012), Linking enclave formation to magma rheology. *Journal of*
428 *Geophysical Research: Solid Earth* 117. doi: [10.1029/2012JB009393](https://doi.org/10.1029/2012JB009393)
- 429 Holtz, F., Sato, H., Lewis, J., Behrens, H., & Nakada, S. (2005), Experimental petrology of the
430 1991–1995 Unzen dacite, Japan. Part I: Phase relations, phase composition and pre-eruptive
431 conditions. *J. Petrology*, 46, 319–337. doi: [10.1093/petrology/egh077](https://doi.org/10.1093/petrology/egh077)
- 432 Humphreys, M., Christopher, T., & Hards, V. (2009), Microlite transfer by disaggregation of
433 mafic inclusions following magma mixing at Soufrière Hills volcano, Montserrat. *Contributions*
434 *to Mineralogy and Petrology*, 157, 609–624. Doi: [10.1007/s00410-008-0356-3](https://doi.org/10.1007/s00410-008-0356-3)
- 435 John, B.E., & Blundy, J.D. (1993), Emplacement-related deformation of granitoid magmas,
436 southern Adamello Massif, Italy. *Geological Society of America Bulletin*, 105, 1517–1541.
- 437 Marsh, B.D. (1989), On Convective Style and Vigor in Sheet-like Magma Chambers. *J.*
438 *Petrology*, 30, 479–530. doi: [10.1093/petrology/30.3.479](https://doi.org/10.1093/petrology/30.3.479)
- 439 Martel, C., Ali, A.R., Poussineau, S., Gourgaud, A., & Pichavant, M. (2006), Basalt-inherited
440 microlites in silicic magmas: Evidence from Mount Pelée (Martinique, French West Indies).
441 *Geology*, 34, 905–908. doi: [10.1130/G22672A.1](https://doi.org/10.1130/G22672A.1)
- 442 Martin, V.M., Pyle, D.M., & Holness, M.B. (2006), The role of crystal frameworks in the
443 preservation of enclaves during magma mixing. *Earth and Planetary Science Letters*, 248, 787–
444 799.
- 445 McLeod, P., & Sparks, R.S.J. (1998), The dynamics of xenolith assimilation. *Contrib Mineral*
446 *Petrol*, 132, 21–33. doi: [10.1007/s004100050402](https://doi.org/10.1007/s004100050402)
- 447 Michel, L., Wenzel, T., & Markl, G. (2017), Interaction between two contrasting magmas in the
448 Albtal pluton (Schwarzwald, SW Germany): textural and mineral-chemical evidence.
449 *International Journal of Earth Sciences (Geol Rundsch)*, 106, 1505–1524. doi: [10.1007/s00531-
450 016-1363-7](https://doi.org/10.1007/s00531-016-1363-7)

- 451 Murphy, M.D., Sparks, R.S.J., Barclay, J., Carroll, M.R., & Brewer, T.S. (2000), Remobilization
452 of Andesite Magma by Intrusion of Mafic Magma at the Soufriere Hills Volcano, Montserrat,
453 West Indies. *J. Petrology*, 41, 21–42. doi: 10.1093/petrology/41.1.21
- 454 Ottino, J.M., DeRoussel, P., Hansen, S., & Khakhar, D.V. (1999), Mixing and Dispersion of
455 Viscous Liquids and Powdered Solids, in: Wei, J. (Ed.), *Advances in Chemical Engineering*.
456 Academic Press, pp. 105–204. doi: 10.1016/S0065-2377(08)60109-X
- 457 Paterson, S.R., Fowler Jr, T.K., Schmidt, K.L., Yoshinobu, A.S., Yuan, E.S., & Miller, R.B.
458 (1998), Interpreting magmatic fabric patterns in plutons. *Lithos*, 44(1-2), 53-82. doi:
459 [10.1016/S0024-4937\(98\)00022-X](https://doi.org/10.1016/S0024-4937(98)00022-X)
- 460 Paterson, S., Memeti, V., Mundil, R., & Žák, J. (2016), Repeated, multiscale, magmatic erosion
461 and recycling in an upper-crustal pluton: Implications for magma chamber dynamics and magma
462 volume estimates. *American Mineralogist*, 101, 2176–2198. doi: 10.2138/am-2016-5576
- 463 Powell, R.L., & Mason, S.G. (1982), Dispersion by laminar flow. *AIChE Journal*, 28, 286–293.
464 doi: 10.1002/aic.690280218
- 465 Reid, M.R., Coath, C.D., Harrison, T.M., & McKeegan, K.D. (1997), Prolonged residence times
466 for the youngest rhyolites associated with Long Valley Caldera: 230Th-238U ion microprobe
467 dating of young zircons. *Earth and Planetary Science Letters*, 150, 27–39.
- 468 Ruprecht, P., & Bachmann, O. (2010), Pre-eruptive reheating during magma mixing at Quizapu
469 volcano and the implications for the explosiveness of silicic arc volcanoes. *Geology*, 38, 919–
470 922. doi: 10.1130/G31110.1
- 471 Ruprecht, P., Bergantz, G.W., Cooper, K.M., & Hildreth, W. (2012), The Crustal Magma Storage
472 System of Volcán Quizapu, Chile, and the Effects of Magma Mixing on Magma Diversity. *J.*
473 *Petrology*, 53, 801–840. doi: 10.1093/petrology/egs002
- 474 Ruprecht, P., & Cooper, K.M. (2012), Integrating the Uranium-Series and Elemental Diffusion
475 Geochronometers in Mixed Magmas from Volcán Quizapu, Central Chile. *J. Petrology*, 53, 841–
476 871. Doi: 10.1093/petrology/egs001
- 477 Ruprecht, P., & Wörner, G. (2007), Variable regimes in magma systems documented in
478 plagioclase zoning patterns: El Misti stratovolcano and Andahua monogenetic cones. *Journal of*
479 *Volcanology and Geothermal Research*, 165, 142–162. doi: 10.1016/j.jvolgeores.2007.06.002
- 480 Sachs, P.M., & Stange, S. (1993), Fast assimilation of xenoliths in magmas. *Journal of*
481 *Geophysical Research: Solid Earth*, 98, 19741–19754. doi: 10.1029/93JB02176
- 482 Shamloo, H.I., & Till, C.B. (2019), Decadal transition from quiescence to supereruption:
483 petrologic investigation of the Lava Creek Tuff, Yellowstone Caldera, WY. *Contrib Mineral*
484 *Petrol*, 174, 32. doi: 10.1007/s00410-019-1570-x
- 485 Sparks, R.S.J., & Marshall, L.A. (1986), Thermal and mechanical constraints on mixing between
486 mafic and silicic magmas. *Journal of Volcanology and Geothermal Research*, 29, 99–124. doi:
487 10.1016/0377-0273(86)90041-7
- 488 Tsuchiyama, A. (1986), Melting and dissolution kinetics: Application to partial melting and
489 dissolution of xenoliths. *Journal of Geophysical Research: Solid Earth*, 91, 9395–9406. doi:
490 10.1029/JB091iB09p09395

- 491 Tsuchiyama, A. (1985), Dissolution kinetics of plagioclase in the melt of the system diopside-
492 albite-anorthite, and origin of dusty plagioclase in andesites. *Contributions to Mineralogy and*
493 *Petrology*, 89, 1–16. doi: 10.1007/BF01177585
- 494 Turner, S., & Costa, F. (2007), Measuring Timescales of Magmatic Evolution. *Elements*, 3, 267–
495 272. <https://doi.org/10.2113/gselements.3.4.267>
- 496 Wiebe, R.A., & Collins, W.J. (1998), Depositional features and stratigraphic sections in granitic
497 plutons: implications for the emplacement and crystallization of granitic magma. *Journal of*
498 *Structural Geology*, 20, 1273–1289. doi: 10.1016/S0191-8141(98)00059-5
- 499 Wiebe, R.A. (2016), Mafic replenishments into floored silicic magma chambers. *American*
500 *Mineralogist*, 101, 297–310. doi: [10.2138/am-2016-5429](https://doi.org/10.2138/am-2016-5429)
501

The Survival of Mafic Magmatic Enclaves and the Timing of Magma Recharge

Philipp Ruprecht¹, Adam C. Simon², and Adrian Fiege³

¹Department of Geological Sciences and Engineering, University of Nevada, Reno, NV, USA.

²Department of Earth and Environmental Sciences, University of Michigan, Ann Arbor, MI, USA.

³Department of Earth and Planetary Sciences, American Museum of Natural History, New York, NY, USA.

Contents of this file

Text S1 to S3

Figures S1

Introduction

The supporting information includes a brief description of the underlying experiments of Fiege et al. (2017) as well as the analytical and image processing of those experimental charges. Moreover, basic observation from these experiments are summarized and connected to mafic enclave textures in natural systems.

Text S1. Summary of and motivation for experiments by Fiege et al. (2017)

We performed a time-series of diffusion couple experiments (1, 10, 79 hrs) of natural basaltic andesite (VQ22A, IGSN: PPRAI100T) and dacites (VQ37D, IGSN: PPRAI101I) from Volcán Quizapu at sub-liquidus conditions. These experiments model to first order the interaction of a highly crystalline basaltic andesite (melt fraction 20-40 vol.%) with nearly aphyric dacite (melt fraction >90 vol.%) a condition frequently found in natural systems in the form of mafic enclaves (e.g., Bacon & Metz, 1984; Clynne, 1999; Browne et al., 2006; Ruprecht et al. 2012). The time series experiments are isothermal (1000 °C) and at a temperature intermediate between potential storage conditions for dacite and basaltic andesite, a condition that is relevant when significant mafic recharge leads to heating and dispersal of enclaves through a dacitic magma chamber (e.g., Clynne, 1999; Browne et al., 2006; Ruprecht & Bachmann, 2010; Ruprecht et al., 2012). Furthermore, experiments were run at isobaric conditions (150 MPa) and volatile

contents consistent with near volatile saturation in both the dacite and the basaltic andesite at the P-T conditions and the emerging crystallinity. A detailed description of the experimental design can be found in Fiege et al. (2017).

Text S2. Analytical procedures and observations

We investigated the textural evolution of the basaltic andesite-dacite interface via x-ray mapping at the electron microprobe facility (Cameca SX-100) of the American Museum of Natural History in New York (Figure S1). The complete data processing was described in Fiege et al. (2017). The phase assemblage (plagioclase, plg; clinopyroxene, cpx; orthopyroxene, opx; Fe-Ti oxides, ox; glass, gl) and relative fractions were quantified using WDX mapping on Ca, Mg, Fe, Al, and K. A composite phase map was produced using all five element maps for these experiments with a specifically developed MATLAB script. While the significant compositional diversity of Fe-bearing phases ensures straight forward determination of the respective phase fractions, distinguishing between plagioclase and glass is more uncertain. The latter being complicated not only by the compositional similarities, but also by the fine-grained nature (<50 microns) of the experimental products. Thus, special care was taken to analyze all time-series experiments with the same protocol. However, minor systematic errors resulting from the image processing are not affecting the outcome of this study as relative variations carry the important information to track the crystallinity evolution near the interface.

Given the nature of the experiments (short duration, no temperature cycling) the basaltic andesite is fine-grained and forms the rigid crystal framework. In naturally occurring enclaves also a fine-grained matrix (resulting from second boiling) constitutes the rigid crystal framework. However, a condition that is distinct in most natural enclaves from the experimental setup is the common presence of large phenocrysts from pre-mixing crystallization in the recharge magma.

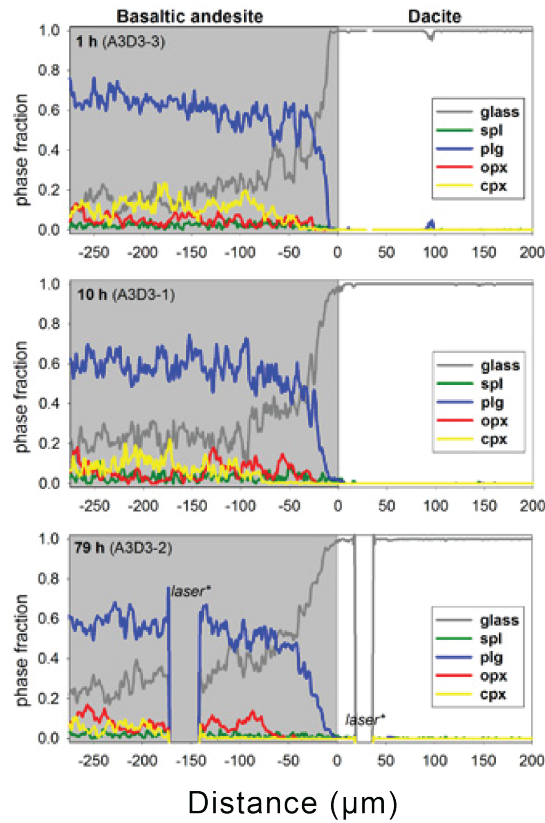
The textural evolution of the run products is straight forward and discussed by Fiege et al. (2017). As the two magmas equilibrate the major phases in the basaltic andesite (plagioclase, orthopyroxene and clinopyroxene) all become consumed through crystal dissolution and the crystal network loosens at the interface.

Text S3. Processing of underlying data to obtain dissolution rate estimates

The underlying data in the form of phase fractions for each experimental run were published in Fiege et al. (2017) as tables S-D2 to D4. This phase fraction data represents the basis for figure 2B and parts of figure 3A in this study. The additional data processing of the phase fraction is provided in an excel sheet stored in the EarthChem library (doi.org/10.1594/IEDA/111480). The glass fractions for the 1, 10, and 79 hr experiments provided by Fiege et al. (2017) as a function of distance from the dacite-basaltic andesite interface are in columns G-L. Since this analysis exclusively focuses on the basaltic andesite part of the experiment we separate this half of the diffusion couple experiment for the three time series experiments in columns N-Q. This unfiltered dataset for the glass fraction is shown in Figure S1 as dotted lines. The noise in this dataset is substantial. Therefore, for the analysis in this contribution melt fractions from Figure S1A were smoothed using a Savitzky-Golay Filtering (second order and 33 elements; Figure S1B, column R-T). Smoothing highlights the continuous increase of melt fraction in the basaltic andesite with time. Minor deviations from a monotonous decrease in melt fraction with distance from the interface is expected in these complex experiments as phase distributions and textures are not perfectly uniform across experimental charges. The nearest intercept relative to the basaltic andesite-dacite interface was selected to determine the rate of melt fraction advancements shown in Figure 2B of the

main text. The advancement of the increase of the glass fraction within the basaltic andesite follows a square-root of time dependence (Figure 2B) that we use to estimate plagioclase dissolution rates in these multi-grain composite samples. By choosing the nearest intercept the resulting diffusion-controlled dissolution rate represents a minimum, which equates to maximum mafic enclave survival times in the model.

A



B

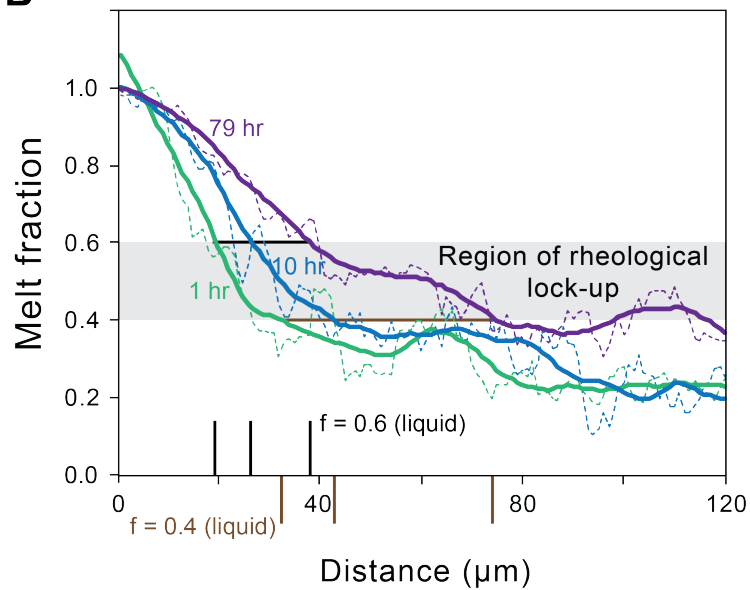


Figure S1. Analysis of advancement of melting front using the experiments of Fiege et al. (2017). A) Originally reported phase fractions for each run average the across the experimental charge modified from Fiege et al. (2017). Phase fractions were averaged perpendicular to the basaltic andesite-dacite interface. B) Smoothed melt fraction curves (solid) and original melt fractions from A (dotted). Smoothing was done using a Savitzky-Golay Filter (second order and over range of 33 datapoints). Melt front advancement is taken as the first intersection of the smoothed curve with the respective melt fraction f . Taking the first intercept represents a minimum diffusion-controlled dissolution rate and therefore, leads to maximum mafic enclave survival times in the model presented in the main text. Corrections for the zero-intercept are ignored as micron-scale localization of the basaltic andesite-dacite interface is limited by the experimental design and minor capsule deformation.